Spectral and angular solar properties of a PCM-filled double glazing unit

Francesco Goia[a,*], Michele Zinzi[b], Emiliano Carnielo[c], Valentina Serra[d]

[a] *The Research Centre on Zero Emission Buildings, Faculty of Architecture and Fine Art, Norwegian University of Science and Technology, Trondheim (Norway)*

[b] *ENEA – Italian National Agency for New Technologies, Energy and Sustainable Economic Development, Roma (Italy)*

[c] *Mechanical and Industrial Engineering Department, Roma Tre University, Roma (Italy)*

[d] *TEBE Research Group, Department of Energy, Politecnico di Torino, Torino (Italy)*

ABSTRACT

Background: Phase Change Materials (PCMs) have been proposed as a means to increase the thermal inertia of glazing systems. These materials have optical features that need to be investigated and characterised in order to better understand the potential of these systems and to provide reliable data for numerical simulations.

Methods: the spectral and angular behaviour of different PCM glazing samples, characterised by different thicknesses of PCMs, were investigated by means of commercial spectrophotometer and by means of a dedicated optical test bed that includes a large integrating sphere with a diameter of 0.75 m. Such equipment was necessary because of the highly diffusive behaviour of the PCM layer when in the solid state of aggregation.

Results: the paper provides a data set of luminous and solar properties of glazing units with PCMs in gaps; the data set uses results from an advanced optical facility that overcomes the intrinsic limitations of commercial spectrophotometers in measuring the optical properties of the advanced transparent materials. In detail, transmittance, reflectance and absorptance spectra of double glazing units with characterized by different PCM layer thicknesses in the gap, measured at different incident beam angles, are reported. Integrated values calculated according to relevant international standards are thus provided. Optical features of PCM glazing systems are also highlighted and issues related to the integration of these systems in buildings are discussed.

Keywords: PCM; advanced glazing; optical properties; large integrating sphere; spectrophotometric analysis; spectral characterisation; angular characterisation.

* *contact author: Francesco Goia; e-mail: francesco.goia@ntnu.no; tel: +47 73550275; fax: +47 73595094.*

1. INTRODUCTION

1.1. Background

Transparent components for the building envelope play an important role in shaping the energy performance and consumption of buildings, affecting thermal losses, solar gains and daylighting availability. Functions provided by efficient glazing systems include high insulation properties [1, 2]; solar and lighting dynamic properties [3]; renewable energy integration [4]; and shading and redirection [5].

Even if several functions can be provided by transparent systems, the thermal inertia is typically a task for the opaque components of the building envelope. The thermal inertia plays an important role, especially in warm climates, modulating solar gains through to the structure mass, but it can also have beneficial effects in increasing the efficiency of passive solar energy exploitation in colder climates. Glazing technologies do not have a significant thermal inertia and instantly transmit the solar gains to the built environment.

Advanced thermally responsive solutions are under investigation, with the objective of increasing the thermal inertia of transparent façades. In particular, the exploitation of the Latent Heat Thermal Energy Storage (LHTES) potential of some materials, known as Phase Change Materials (PCMs) [6, 7], is gaining popularity within the building industry, with several trends in research and development [8–10] that include the adoption of PCMs in transparent components.

The insertion of PCMs in semi-transparent or transparent components has been proposed since the eighties (e.g. [11, 12]; as cited in [13], a patent on a transparent PCM-based system [14] can also be found), but has received less attention than other PCM applications in non-transparent elements. Contrary to opaque PCM-based components, the melting process of a PCM in a partially transparent container is enhanced by the absorption of solar irradiation throughout the whole layer [15]. The aim of the PCM glazing concept is thus to absorb part of the solar radiation for thermal energy storage purposes while letting (part of) the visible radiation enter the indoor environment for daylighting. The optical properties of many PCMs are therefore used to selectively take advantage of the different features of solar radiation in order to create a building envelope component with a (relatively) high heat capacity (something unusual in glazing systems) together with transparency in the visible spectrum. Reliable information on the optical properties of PCMs employed in semi-/transparent components is therefore of fundamental importance for the development of this type of façade component, which has started to appear on the market (e.g. [16]).

So far, the evaluation of the impacts of PCM-based technologies on the energy performance of the building has been mostly carried out by means of experimental activities [13, 17–19]. However, although experimental

measurements provide very detailed information, the generalisation of such outcomes is often not straightforward. Instead, the development of dedicated numerical simulation tools may allow more extensive analyses to be carried out, as well as optimisation of the PCM-based glazing to be done according to different applications, boundary conditions and climates.

1.2. Aim of the research activity

At present, it is not easy to get access to a full data set that shows the optical properties of PCM layers. Though some research activities on this topic have been carried out in the past (cf. Section 2), very little data concerning the optical properties of such materials can be found in the literature making it difficult to carry out reliable simulations of these systems. Therefore, the research activity presented in this paper deepens the understanding of the influence of a PCM layer on the optical (solar and visual) properties of glazing systems, and aims to obtain a useful data set for numerical thermal and lighting simulations of PCM-based glazing systems, such as [20]. In order to reach this goal, different thicknesses of PCMs are used in this investigation, as well as different impinging beam angles, so that the impacts of such variables are also considered. Data collected by means of dedicated laboratory analyses and presented here can be used in future research activities where PCM glazing systems are simulated and the optimal configuration is researched for each climate or context (e.g. type of building, orientation, internal load).

It is important to underline that this work places the focus on the behaviour of PCM layers when in the solid state, and this is due to two main reasons. First of all, the behaviour of the material when solid is less conventional and more complicated to characterise than that of the liquid state. In fact, when in liquid state, most PCMs behave as conventional transparent components, with dominating direct-to-direct transmission mode, while these materials show high scattering phenomena when in solid state. Secondly, the use of PCMs in the transparent component is meaningful if the material does not completely change its state of aggregation (from solid to liquid) and remains in the transition phase, where the optical appearance and properties are very similar to those of the solid state. In fact, as demonstrated in previous research activities (e.g. [18, 19]), when the entire phase change is exploited, the energy and comfort performance of PCM glazing systems becomes worse than other more conventional systems. Therefore, during the design phase, the choice of the PCM transition temperature, the amount of material and in general the layout of the glazing system must be selected so that a complete transition to the liquid phase is (almost) always avoided and the PCM layer stays (most of the time) in the transition phase. From this perspective, the characterisation of the solid state becomes more useful than that

of the liquid state, as the PCM glazing systems should primarily present the properties of the solid state during most of its functioning.

2. STATE OF THE ART OF OPTICAL CHARACTERISATION OF PCMs

The oldest record [15] that can be found in the literature on the optical properties of a PCM for application in a semi-/transparent system deals with research-grade, 99 % purity n-Octadecane, a paraffin wax with a straight-chain alkane, $CH_3(CH_2)_{16}CH_3$, a material with a nominal melting temperature in the range 28–30 °C and a latent heat of fusion of about 230 J/g. Only the spectral absorption coefficient can be found in that publication.

Ten years later, Manz et al. [13] investigated a commercially available salt hydrate PCM, $CaCl_2 \cdot 6H_2O$ (with additives of approximately 5 % of the mass). This material shows a latent heat of fusion of approx. 190 J/g, a nominal melting temperature of approx. 27 °C and small supercooling effects (1–3 °C); its thermal reliability was assessed [21] and found to be stable after thousands of cycles. The experimental apparatus for the characterisation of optical properties was a Perkin Elmer Lambda 7 spectrophotometer equipped with an integration sphere of 150 mm in diameter, and the range 350–2500 nm was investigated. The PCM was incorporated in a glass vessel and the spectral transmittance and reflectance (direct-to-hemispherical) of two samples (one with a thickness of 10 mm and the other 20 mm) were measured at two temperatures: 20 °C (solid state) and 35 °C (liquid state). Furthermore, the distribution of light scattered when the PCM is in solid state was measured by means of a laser beam in a 1.5 mm thick PCM sample, and a narrow, forward-oriented distribution of scattered light was found. Finally, the refractive index was measured in an Abbe refractometer. As far as the liquid state is concerned, the spectral absorption coefficient was calculated neglecting scattering effects, while as far as the solid state is concerned, the global reflectance, absorptance and transmittance of the PCM layer were calculated by means of Montecarlo simulations, assuming randomly oriented scattering particles. Unfortunately, the paper does not contain details about the measured/calculated reflectance, absorptance and transmittance for the liquid or the solid state, but reference is given [22].

Weinläder et al. [18] carried out a detailed investigation into the optical properties of different PCM substances: a commercial-grade paraffin wax and two salt hydrates (not commercially available at the time of the publication).

The paraffin wax had a nominal melting temperature of approx. 25 °C and a latent heat of fusion of approx. 150 J/g; the first salt hydrate was $CaCl_2$ $6H_2O$, the same investigated in [12, 17], while the second one was based on a lithium nitrate ($LiNO_3$ $3H_2O$) and showed latent heat of fusion of approx. 270 J/g and a nominal melting temperature of about 30 °C. The measurements were carried out by means of two different devices:

UV/VIS/NIR transmission and reflection spectra (250–2500 nm) were collected with a Lambda-9 spectrophotometer equipped with a 6 cm diameter integrating sphere; due to the elevated scattering effects, additional investigations were carried out on the VIS/NIR spectra (400–2000 nm) with a spectrophotometer equipped with an integrating sphere of 70 cm in diameter. Finally, the directional distribution due to scattering effects was evaluated by means of a monochromatic source light (543 nm) and a movable photodiode in the angle range -60/+60 deg. [23]. The paper [18] reports that all the materials have equally high transmittance in the visual range (approx. 0.9), which decreases to about 0.5 with the paraffin wax showing lower absorption than the salt hydrates. More detailed information is given in [23], where the evaluation of the complex spectral refractive indices is presented from transmittance and reflectance measurements for various thicknesses, as well as the mean effective scattering coefficients from transmittance measurements.

Recently, Gowreesunker et al. [24] performed an investigation on a paraffin wax whose nominal melting temperature was 27 °C and with a latent heat of fusion of approx. 180 J/g (a material very similar to the organic PCMs analysed in [15, 18, 23]). The characterisation campaign was carried out, in the wavelength range of 200–1600 nm, with a Perkin Elmer Lambda 1050 spectrophotometer, which recorded the transmission spectrum. A dedicated experimental apparatus was then conceived in order to both maintain the sample at the desired temperature and to take into account the scattered radiation – a phenomenon that cannot be caught by conventional spectrophotometers. It was made up of a 150 W metal halide (iodide discharge) lamp (spectrum approx. 350–850 nm) used as a light source, a reflector casing (a square-section duct with internal walls covered with reflective aluminium foils) that hosted the sample, and a Kipp & Zonen CMA-6 pyranometer placed at the end of the casing measuring the radiation heat flux (W/m^2) transmitted through the glazed surface test specimen. The PCM was incorporated in ordinary double glazing, 20 x 20 cm, consisting successively of 4 mm glass, 16 mm PCM layer and 4 mm glass, and the grey radiation transmittance measured for different temperatures – and thus different balances between liquid and solid fraction, from fully solid to fully liquid PCMs. Considering that the refractive indices of the glass and the paraffin wax were very close (in the range 1.4–1.5), the researcher inferred that the effects of internal reflections in the system PCM-glass were of minimal consequence. Hence, the overall radiation attenuation effects were only due to the reflection at the primary air/glass interface and to the absorption in the PCM (and glass) layer. This way it was possible to later derive the scattering (σ_s) and absorption (σ_a) coefficients for a 16 mm PCM layer under different temperatures (and thus liquid/solid fraction).

3. MATERIALS AND SAMPLES

Several samples have been made in order to characterise the optical properties of paraffin wax layers placed in the gap of a DGU (Double Glazing Unit). A total of six samples were made, combining different PCM layer thicknesses with different paraffin waxes: three thicknesses were used (6, 15 and 27 mm) in combination with two paraffin materials (RT 21, a paraffin wax that presents a nominal melting temperature of 21 °C, and RT 35, a paraffin wax with a nominal melting temperature of 35 °C).

The glass panes employed were made of extra-clear glass (4 mm thickness), whose optical properties are reported in Table 1.

Table 1

The reason for using two paraffin waxes with different melting temperature is due to the fact that it was necessary to ensure that the paraffin wax did not change its state of aggregation during the measurement, nor that it could be in the phase change range. Considering that experiments were carried out at ambient air temperature during relatively mild summer days (air temperature in the range 24–28 °C), it was assured that neither the RT 21 nor the RT 35 were in the middle of the transition phase and that the largest amount of each paraffin wax was in complete liquid state or in complete solid state respectively. Samples with RT 21 were thus used to characterise the optical properties of liquid-state paraffin wax, while samples with RT 35 were used to measure the solid-state properties.

It was possible to adopt such a procedure since no differences in the optical behaviour are expected between two paraffin waxes that have a nominal melting temperature in a relatively close interval (approximately 15 °C). In fact, the two materials – a mixture of waxes with a majority of n-Heptadecane ($C_{17}H_{36}$) and n-Nonadecane ($C_{19}H_{40}$) for RT 21 and RT 35 respectively – show a very similar structure, i.e. a straight-chain alkane with a different length. While this small difference is enough to deeply affect some thermal properties of the components (i.e. the phase change range and, to a lesser extent, the latent heat of each phase change), the optical properties do not change considerably. In fact, the dimension, geometries and features of the molecules are the same for both the materials and thus do not lead to different properties. It is therefore reasonable to assume that there is no change in the macroscopic optical properties of the two paraffin layers.

The samples used for the characterisation had a gross frontal area of 25 cm x 25 cm, while the net area that can be used to measure the optical properties was 21 cm x 21 cm. This dimension was selected according to the testing equipment geometry. In Figure 1, two samples among those used in this experimental campaign are shown and the light transmission mode features can be seen: when the PCM is in solid state (sample on the left),

the dominant transmission mode is direct-to-diffuse, while when the paraffin wax is liquid (sample on the right), direct-to-direct transmission takes place.

Figure 1

4. EQUIPMENT AND PROCEDURES

The experimental analysis was carried out in two different steps. The samples were first characterised using a commercial spectrophotometer, and next they were measured using an experimental facility whose configuration allows more accurate measurement of diffusing and scattering materials to be done, as well as off-normal incident radiation analyses. The experimental facilities are described below.

4.1. Spectrophotometric measurements

The first set of measurements was carried out with a Perkin Elmer Lambda 950 commercial double beam type spectrophotometer. Measurements were carried out in the whole solar range, between 300 and 2500 nm, with a 5 nm spectral resolution. The slit aperture was set to 2 nm in the visible range and in servo mode in the near-infrared range, the latter being a dynamic operation mode that varies the slit aperture as a function of the optimal energy input at every wavelength. Normal direct and hemispherical transmittance and reflectance measurements were performed. Dedicated accessories were mounted for the direct measurements, while a Spectralon-coated 15 cm diameter integrating sphere was used for the hemispherical measurements. The reflectance measurements, carried out at an angle of incidence of 6 °, were performed versus a calibrated aluminium reference for the direct component and versus a calibrated white reference for the hemispherical quantity.

Due to the dimensions of the samples (25 x 25 cm), they could not be placed in the standard compartments and precautions were taken in order to preserve the accuracy of the measurements. The instrument accuracy is 0.01, without taking into account the uncertainties introduced by the sample to be tested.

The instrument was used to perform transmittance and reflectance measurement of the DGU with a 15 mm gap in the following configurations: without PCM in the gap; liquid-state PCM in the gap; solid-state PCM in the gap. The solar and luminous quantities are calculated starting from the spectral data using the reference solar spectrum defined in ISO 9050:2003 [25].

4.2. Large diameter integrating sphere measurements

Because of the thickness and geometry of the samples, as well as their scattering properties, the commercial spectrophotometer measurements were coupled to a measurements campaign carried out by means of a large

dimension optical facility, whose characteristics are described in detail in Maccari et al. [26]. The main features of the optical bench are as follows:

- It has a tungsten halogen lamp with adjustable power, ranging from 250 up to 1000 W. The size of the collimated beam can be modulated through a system of lenses and diaphragms according to the measurement requirements. Usual beam diameters range from 4 to 10 cm.
- The light source in transmittance is mounted on a holder, the arm of which can rotate in order to vary the angle of the incident radiation and perform off-normal measurements.
- The sample is mounted inside the sphere on a holder, which can rotate on a vertical axis in order to perform off-normal absorptance measurements.
- It has an integrating sphere with a 75 cm diameter, an external shell made of aluminium and an internal surface made of Spectralon, a white material with reflectivity greater than 95 % in the whole solar range (300–2500 nm). The sphere is equipped with several ports and a central sample holder; the layout of the facility can be adjusted to perform transmittance, reflectance and absorptance measurements.
- Finally, the detection system consists of three array spectrometers and three detectors: NMOS for the 250–1000 nm range (dispersion 1.4 nm/pixel); InGaAs for the 900–1700 nm range (dispersion 3.125 nm/pixel); ExtInGaAs for the 1600–2500 nm range (dispersion 3.52 nm/pixel).

Figure 2

Figure 2 shows the experimental facility in the transmittance and reflectance measurement modes. Spectral transmittance, reflectance and absorptance measurements were performed on the selected samples. Being of the single beam type, the transmittance and reflectance measurements were corrected with the auxiliary port method [26]. The measurement procedures are described below.

- *Transmittance mode.* The sample port is 20 cm in diameter and the incident beam diameter is 6 cm. The transmittance is measured as the ratio of the energy transmitted by the specimen mounted on the sample port on the energy directly entering the sphere; see Figure 2. The measurements are performed at the following incidence angles: 0, 30, 45 deg.
- *Reflectance mode.* The sample port is 20 cm in diameter and the incident beam diameter is 6 cm. The radiation enters the sphere through a port facing the sample port and hits the sample with an 8 deg. angle of incidence. The reflectance is measured as the ratio of the energy reflected by the specimen mounted on the sample port and the energy entering and hitting the sphere wall directly. Only the near-normal incidence reflectance is carried out.

- *Absorptance mode.* The sample port is 12 cm in diameter and the incident beam diameter is 6 cm. The radiation enters the sphere through the sample port and hits the sample mounted inside the sphere with a suspended rod. The absorptance is measured as the complement to one of the ratios between the energy measured when the beam hits the sample and the energy entering and hitting the sphere wall directly. The measurements are performed at the following incidence angles: 8, 30, 45 deg.

Angular-dependent measurements were carried out up to 45 deg.; higher incidence angles were not tested because of the high scattering behaviour of the sample, which did not allow accurate measurements above that value. The instrument error was estimated to be 0.02 for the different measurement modes. Measurements were performed between 400 and 2000 nm, covering 93 % of the whole solar spectrum energy. The solar quantities were calculated starting from the spectral data using the reference solar spectrum defined in ISO 9050:2003 [25].

5. RESULTS

5.1. Spectral profiles and integrated coefficients with commercial spectrophotometer

As previously mentioned, the PCM used in the prototypes has, in the liquid phase, a fully – transparent – regular behaviour and it can therefore be efficiently characterised by means of conventional spectrophotometers. Focus is thus placed on the results for the material in the solid state, when it exhibits a diffusing behaviour.

As far as the measurements carried out with commercial spectrophotometers are concerned, they were first carried out with the instrument equipped with the accessories to measure the direct components of the reflectance and transmittance on the PCM in the solid state. Due to the high scattering behaviour of the sample, the direct transmittance ($\tau_{v\rightarrow}$, $\tau_{e\rightarrow}$) is zero across the whole spectral range, and hence no regular components are observed for the three glazing units. The direct reflectance luminous and solar quantities ($\rho_{v\rightarrow}$, $\rho_{e\rightarrow}$), calculated according to the procedures defined in [25], are reported in Table 2. In particular, due to the similar refractive index of the clear glass pane and the PCM, the specular reflection is given only by the interface between the air and the first glass pane. Hence, specular reflectance is independent from the thickness of the PCM layer.

Later, measurements were carried out with the 150 mm integrating sphere to measure the (near) normal hemispherical transmittance and reflectance as well. Broad-band values were then calculated and they are presented in Table 2. Spectral hemispherical reflectance and transmittance for the three DGUs with different PCM layer thicknesses are plotted in Figures 3 and 4 for the PCM in the solid state using the commercial spectrophotometer apparatus. Broad-band values of hemispherical reflectance and direct-to-hemispheric transmittance are presented in Table 2 too.

Figure 3

Figure 4

Table 2

It is important to underline in this section that the transmission and reflection coefficients measured by means of the commercial spectrophotometer are low in contrast with basic observations of the component in practice and from experimental analyses [18]. With this set-up, the absorptance appears to be the dominant feature in both the visible and infrared (IR) range. This effect takes place because the high scattering phenomena cannot be fully and efficiently tackled by means of conventional spectrophotometer and a more advanced test rig is necessary to fully characterise the behaviour of the PCM layer when in the solid state. It is therefore necessary to perform the optical characterisation using a large integrating sphere apparatus for more detailed and reliable data, especially as far as the solid state of the DGU PCM is concerned.

5.2. Optical measurements with a large diameter integrating sphere facility

5.2.1. Spectral profiles

In Figures 5, 6 and 7, the spectral transmittance (τ), reflectance (ρ) and absorptance (α) of the PCM glazing samples are shown respectively – left: spectra of the 15 mm thick DGU PCM, with PCM in liquid state (dashed line) and in solid state (solid line); right: spectra of the DGU PCM with 6 mm, 15 mm and 27 mm thick PCM, for the solid state of aggregation only.

In Figure 5, the relevant difference in the transmission feature of the DGU PCM, when the PCM is in liquid state and in solid state, can be seen. While the two spectra show a very similar profile (i.e. an almost constant transmittance in the visible range, and a more selective behaviour in the near-IR range), a considerable change in the transmittance value is seen. The selective behaviour in the near-IR range is almost identical for the two states of aggregation, meaning that this feature is only related to the nature of the material (a paraffin wax) and independent of the state of the PCM. This result is in line with the expected behaviour, since spectral absorption bands in the near-IR range are due to the chemical structures of the PCM (C-H bonds), which remains the same in both states of aggregation.

As far as the influence of the different thickness is concerned (Figure 5), it is possible to see that this parameter affects the transmittance to a certain extent, but spectra are very similar – as also revealed by the spectrophotometric analysis with a commercial spectrophotometer (see 5.1). The transmittance of the 15 mm

sample seems to be higher than that of the 6 mm sample, in the range 600–1200 nm – this aspect is elaborated upon in the Discussion section. Most of all, it is noticeable that the transmittance spectrum recorded by means of the large integrating sphere is far higher than that recorded by the commercial spectrophotometer (compare Figures 3 and 5), which is not fully capable of recording the transmitted energy in the direct-to-diffuse mode.

Figure 5

Figure 6

Figure 7

When the PCM is in the solid state, the reflectivity of the system is far higher (up to three times) than when it is in the liquid state (Figure 6). Moreover, the liquid state profile is flatter and more constant (reflectance is approx. 0.1 for a 15 mm thick PCM layer) in all the visible and near-IR spectra, while the profile of the solid state shows a decreasing value, moving from the visible to the near-IR spectrum, due to the high selective absorptance in the near-IR region. For a wavelength higher than 1700 nm, the system shows a constant behaviour, regardless of the state of aggregation.

The thickness of the PCM layer has a low impact on the reflectivity (Figure 6): the thinnest PCM layer has the highest reflectivity, while the other two configurations have almost the same profile. Once again, it is possible to underline the difference between the analysis carried out with and without the large integrating sphere: reflectivity measured with an appropriate test rig (suitable for highly diffusive materials) reveals it to be approximately three times that measured by means of conventional test bed (compare Figures 4 and 6). This occurs because of the non-specular feature of the materials, which appears to have an almost Lambertian behaviour.

The absorption coefficient of the solid PCM is much higher than that of the liquid PCM (Figure 7), but the spectral profiles are again very similar for the two states of aggregation with common selective absorption bands (900 nm, 1200 nm and 1400 nm). Greater PCM thicknesses imply higher absorption coefficients, but as in all the other cases, the PCM thickness does not affect the spectral profile.

5.2.2. Integrated coefficients

Spectra recorded with the large integrating sphere test rig have been integrated according to ISO 9050:2003 in order to obtain integral values. In Table 3, transmittance, reflectance and absorptance are summarised for the visible (*v*), near-infrared (*nir*) and solar (*e*) spectra for different thicknesses of the PCM layer, both when the

PCM is fully liquid and fully solid. The sum of the transmittance, reflectance and absorptance integral coefficients may differ from 1 because of the measurement uncertainties.

Table 3

The average percentage error on the sum of the τ, ρ, α coefficient is 2 %, with a maximum value of 4 % (visible spectrum, sample with PCM layer of 27 mm thickness). A deeper analysis on the measurement accuracy and limitation of the test rig is presented in the Discussion paragraph.

5.2.3. Angular characterisation

The angular behaviour of the DGU PCM is also investigated, with measurements for transmittance (Figures 8 and 9) and absorptance (Figure 10) for both the solid and liquid state with different incident beam angles (up to 45 deg.). In Table 4, the results concerning the solid state of the 15 mm PCM layer are presented. In Table 5, the angular transmittance (in the different spectra) is reported for different thicknesses of PCM. The behaviour of the system when in liquid state has been investigated only for the 15 mm PCM layer because the PCM shows conventional behaviour when in the liquid state.

As far as the angular characterisation is concerned, it is possible to state that the PCM layer has, even when in solid state, a conventional dependence on the beam angle, at least in the range 0–45 deg.: reflectance and absorptance increase as the beam angle increases, while transmittance decreases – regardless of the investigated spectrum.

Figure 8

Figure 9

Figure 10

Table 4

Table 5

6. DISCUSSION

6.1. Optical behaviour of the PCM glazing systems

The optical characterisation of the selected samples provides a detailed data set of optical properties, as well as details about the technology and design input for numerical lighting and thermal analyses, which are necessary for the building integration assessment. It is worth noting that luminous quantities can be directly used for

analysis and design, while solar properties need to be merged with other thermal properties to take account of the heat storage and release phenomena.

The results show that the material passes from a regular behaviour in the liquid phase to a full diffusing behaviour in the solid state, with no regular transmittance component recorded. The light transmittance in the solid state is about 50 % for the three samples, which though lower than an equivalent DGU without PCM in the gap, still provides adequate daylighting. Moreover, the PCM has high scattering/diffusing properties in the solid state, thus providing more uniform lighting distribution inside the building. This aspect needs further investigation: experimental or numerical bi-directional scattering functions for PCMs in the solid state might provide additional information about the daylighting and visual comfort in buildings equipped with transparent PCM components.

The selected samples present characteristics in the liquid state that are similar to conventional DGUs in the visible range due to the high transparency in the aggregation state. However, the inclusion of paraffin waxes determines some selectivity in the near-IR range: the light transmittance to solar transmittance ratio is 1.13 for the PCM samples, while a conventional DGU (assembled with extra-clear glass panes as was for the PCM DGU) has a ratio of approx. 1. The light transmittance to solar transmittance ratio rises to 1.2 for the three samples in the solid state. Even if these figures are far lower than those of solar control glazing units (e.g. light transmittance to solar transmittance ratio can be higher than 2 in modern glazing), the PCM DGU exhibits selective properties in both aggregation states.

The comparison between the commercial spectrophotometer and the large integrating sphere facility results shows how the former does not provide reliable results. This apparently trivial finding highlights the problem of how existing standards and conventional instruments can mislead the final users regarding characterisation of advanced components and how properties need to be characterised and communicated for daily use in design by practitioners.

6.2. Evaluation of the experimental procedures and equipment and limitations in the analyses

The results of the experimental activities point out that particular care must be paid when dealing with the characterisation of advanced glazing systems which do not show a conventional behaviour. In particular, the use of a commercial spectrophotometer to evaluate the optical properties of PCM glazing is revealed to be completely inadequate because this facility is not capable of recording electromagnetic radiation that is transmitted in a direct-to-diffuse mode. In the tested samples, this is the dominant mode, as revealed by the

deeper analysis where spectra recorded by means of the test bed equipped with the large integrating sphere are compared with those obtained by the commercial spectrophotometer.

As far as the measurement accuracy is concerned, it is remarkable that when the test bed equipped with the large integrating sphere is used the sum of the measured integral coefficients, regardless of the spectrum that is recorded, is only 4 % (maximum error) higher than the theoretical value (i.e. $\tau + \rho + \alpha = 1$) for all the tested samples ($\delta = 6$, 15, 27 mm); the average error considering all the spectra and samples is ± 2 %.

This value indicates the accuracy and reliability reached by the experimental equipment, though the paraffin wax also shows a very high scattering behaviour and non-homogenous features.

In particular, it has been noticed that crystalline structures may appear within a more homogenous matrix in the solidification process. As also highlighted during an experimental campaign of a full-scale PCM glazing prototype [19], the re-solidification processes depend on several factors, ranging from macroscopic elements (such as a frame or a shadow) to microscopic components/impurities within the PCM layer that may act as nucleating agents.

These phenomena, affecting the kinetics in the solidification process, determine a different appearance of the PCM layer after every melting/re-solidification cycle, and may lead to difficulties in test–retest reliability, even on the same sample. In fact, the optical behaviour in transmittance/absorptance/reflectance mode can vary quite considerably when a homogenous or crystalline area is hit by the spectrophotometer beam.

This behaviour is visible comparing the transmittance spectra of the 15 mm PCM sample with that of the 6 mm PCM sample – in the 600–1200 nm range, the transmittance of the 15 mm PCM sample is higher than that of the 6 mm sample, a behaviour that is in contrast with physical laws and observations, provided that the two PCM matrices under measurement have the same appearance. However, it has been observed that the 6 mm PCM sample often showed a crystalised area at the centre of the measurement area, probably due to slightly different kinetics of re-solidification. Since the crystalline structures have higher reflectance/absorbance than the homogenous amorphous PCM matrix, the reading of the transmittance 6 mm PCM layer appeared to be affected by this phenomenon.

In order to limit such influence, it is advisable:

- to repeat the measurement several times, each one after a different melting/re-solidification cycle under diverse boundary conditions, and take into consideration the statistical distribution of the recorded values; and

- to select a beam size adequate to hit a representative area of the PCM matrices that can be found in the sample, which is a function of the successive melting/re-solidification phenomena.

As far as the second suggestion is concerned, it is also necessary to point out that large ray beams show contradictory features (there must be a correlation between the beam diameter and the sphere port diameter); if on the one hand the adoption of very large diameter rays would be beneficial, on the other hand it might determine accuracy uncertainties that exceed those caused by using small beams. In particular, angular characterisation becomes particularly tricky when large beams are adopted because a (large) part of the impinging radiation may be scattered and not cross the sphere port, thus resulting in an inaccurate measurement.

In the present work, angular characterisation has been carried out for impinging angles of up to 45 deg., while a full set of measurements would require an angle of incidence higher than 45 deg. However, the experimental facility did not allow higher incidence angle testing because of geometric and materials restraints, depending on the diffusing behaviour and the size of the PCM layers as well as the optical facility configuration.

6.3. Considerations on the integration of PCM glazing systems in buildings

Aside from the discussion about the optical properties of PCM glazing systems, the integration of PCM-based glazing units to building is a relevant issue and it is therefore worth analysing the pros and cons of the adoption of this technology in buildings.

It is important to note, as preliminary considerations, that this solution should not be applied to conventional windows for residential buildings but mainly on commercial buildings, characterised by large glazed façades (and roofs) with high solar gains and low thermal inertia. Reduction and/or modulation of solar gains are a primary strategy to reduce the cooling energy demand and improve thermal comfort conditions. Moreover, the time-shift of solar gain may also be useful for solar energy exploitation for heating purposes, since the day/night mismatch between solar energy availability and heating demand is one of the factors that limit the effective use of passive solar heating in buildings.

Moreover, as mentioned in the Introduction, it is also important to underline that PCM glazing systems can be effective only if the PCM remains in the transition phase for most of the time. In fact, outside the transition phase, the properties (mostly the specific heat capacity) of such materials are not much better than those of other elements (e.g. air layer) used in conventional glazing systems and may lead to an overall worse behaviour.

However, glazing systems based on this PCM can find marketable margins in commercial buildings because there is potential for energy saving and enhanced comfort conditions (especially when the PCM is in solid/transition phase) due to:

1. good daylight;
2. light transmission mostly in the diffuse mode, which reduces glare discomfort and improves light distribution;
3. the exploitation of the latent heat of fusion of the PCM and of the optical absorptivity and reflectivity, and therefore a reduction and time shift of the peak of solar gains; and
4. an increase in the thermal mass of the building (and in particular of the building envelope) compared to other fenestration systems, which still provides the perception of "lightness", transparency and light transmission (important aesthetic issues in commercial buildings).

In previous studies on a simple PCM glazing prototype [18, 19] in a relatively warm climate, it has been shown that a 15 mm layer of PCM can reduce the solar load by one-third, and if coupled with suitable night-time ventilation strategies, even up to 50 % of the daily solar gain can be avoided, still allowing good exploitation of natural light. Moreover, the system also showed improvements as far as thermal comfort is concerned, reducing the risk of discomfort during the summer and winter period.

By contrast, some of the PCM characteristics also represent limits to the diffusion of this technology:

1. the view through the PCM layer is only possible when the PCM is completely liquid – this limits the adoption of PCM windows to certain applications, where viewing the exterior is not a key feature, while large use of PCM glazing in residential buildings appears to not be realistic;
2. the incorporation of a PCM layer increases the weight of the window and problems may arise when large glazing areas are adopted; and
3. the change in the volume between solid and liquid state (even if relatively small, i.e. less than 10 %) is also a challenge that must be properly addressed for successful application of this technology.

One last relevant issue is that PCM glazing systems cannot be directly compared with other conventional and advanced glazing units. PCM glazing systems are characterised by specific thermal and solar properties (namely U and g values) and no thermal capacity, which allows the energy performance of the windows to be assessed and compared. Windows and glazing products are selected by end users on the basis of such properties, and are measured and/or calculated in standard conditions. The definition of those properties does not apply to PCM glazing units because of the thermal capacity behaviour and the non-linear behaviour of the properties. Therefore, new procedures and standards are needed to adequately take into account the performance of this product category and be able to compare it with other solutions available on the market.

7. CONCLUSION

462 The spectral and angular characterisation of glazing systems that include PCM layers is presented in the paper.
463 Spectral τ, ρ, α of different PCM glazing samples (with PCM layers of 6, 15 and 27 mm) have been measured by
464 means of conventional spectrophotometer and of a dedicated test bed equipped with a large integrating sphere.
465 Both the liquid and the solid state of aggregation of the PCM (a paraffin wax) have been investigated.
466 The measurement range was 400–2000 nm, thus covering 93 % of the entire solar spectrum energy.
467 Integrated quantities have then been calculated starting from the spectral data by means of the reference solar
468 spectrum defined in ISO 9050:2003.
469 The experiments have pointed out the highly diffusive behaviour of the PCM layer, with increasing weight of
470 the direct-to-diffuse transmission mode as the PCM layer thickness increases.
471 Such a characteristic requires dedicated measurement facilities to be employed using a spectrophotometer
472 with a large integrating sphere capable of collecting the entire transmitted/reflected quota because the
473 conventional experimental set-up is not suitable and accurate enough to characterise advanced components.
474 Limitations of the measurement procedures and test bed have also been presented, highlighting the capability
475 of the selected instrumentation to characterise the behaviour of PCM glazing. Moreover, opportunities (e.g. good
476 daylight gain and low glare risk, reduction and time-shift of solar gain) and drawbacks (e.g. increased weight,
477 volume change and translucent aspect) of integration of PCM glazing systems in buildings have been illustrated.
478 New configurations of PCM glazing systems can now be simulated using the data set of optical properties
479 presented in this paper and optimisation of such a component can be carried out for different boundary
480 conditions, such as climate or building types.

481 **AKNOWLEDGMENTS**

482 This research was started in the framework of PRIN 2007 – Progetti di Rilevante Interesse Nazionale – funded
483 by the Italian Ministry of Education, University and Research. It is now being continued in the frame of
484 “SMARTglass”, a “Polight” project funded by the Regione Piemonte in 2010. The Research Centre on Zero
485 Emission Buildings of the NTNU is gratefully acknowledged.

REFERENCES

[1] B.P. Jelle, A. Hynd, A. Gustavsen, D. Arasteh, H. Goudey, R. Hart, Fenestration of today and tomorrow: A state-of-the-art review and future research opportunities, Sol Energy Mater Sol Cells 96 (2012) 1–28. DOI: 10.1016/j.solmat.2011.08.010.

[2] R. Baetens, B.P. Jelle, A. Gustavsen, Aerogel insulation for building applications: A state-of-the-art review, Energy Build 43 (2011) 761–769. DOI: 10.1016/j.enbuild.2010.12.012.

[3] R. Baetens, B.P. Jelle, A. Gustavsen, Properties, requirements and possibilities of smart windows for dynamic daylight and solar energy control in buildings: A state-of-the-art review, Sol Energy Mater Sol Cells 94 (2010) 87–105. DOI: 10.1016/j.solmat.2009.08.021.

[4] B.P. Jelle, C. Breivik, H. Drolsum Røkenes, Building integrated photovoltaic products: A state-of-the-art review and future research opportunities, Sol Energy Mater Sol Cells 100 (2012) 69–96. DOI: 10.1016/j.solmat.2011.12.016.

[5] H. Koster, Dynamic daylighting architecture, Birkhauser, 2004. ISBN: 3-7643-6729-6

[6] R. Baetens, B.P. Jelle, A. Gustavsen, Phase change materials for building applications: A state-of-the-art review, Energy Build 42 (2010) 1361–1368. DOI: 10.1016/j.enbuild.2010.03.026.

[7] L.F. Cabeza, A. Castell, C. Barreneche, A. de Gracia, A.I. Fernández, Materials used as PCM in thermal energy storage in buildings: A review, Renew Sustain Energy Rev 15 (2011) 1675–1695. DOI: 10.1016/j.rser.2010.11.018

[8] R. Parameshwaran, S. Kalaiselvam, S. Harikrishnan, A. Elayaperumal, Sustainable thermal energy storage technologies for buildings: A review, Renew Sustain Energy Rev 16 (2012) 2394–2433. DOI: 10.1016/j.rser.2012.01.058

[9] E. Osterman, V.V. Tyagi, V. Butala, N. Rahim, U. Stritih, Review of PCM based cooling technologies for buildings. Energy Build 49 (2012) 37–49. DOI: 10.1016/j.enbuild.2012.03.022.

[10] N. Soares, J.J. Costa, A.R. Gaspar, P. Santos, Review of passive PCM latent heat thermal energy storage systems towards buildings' energy efficiency, Energy Build 59 (2013) 82–103. DOI: 10.1016/j.enbuild.2012.12.042

[11] A.V. Sedrik, Translucent phase change material thermal storage system, In: Proc. 5th Natl. Passiv. Sol. Conf., Newark, DE (USA): 1980, 980–984.

[12] E. Korin, D. Pasternak, E. Rappeport, A. Roy, D. Wolf, A novel greenhouse concept using phase change materials in walls and roof, In: INTERSOL 85 Proc. 9th Bienn. Congr. ISES, Montreal (Canada): 1985, 621–625.

[13] H. Manz, P.W. Egolf, P. Suter, A. Goetzberger, E. Abel, TIM – PCM external wall system for solar space heating and daylighting, Sol Energy 61 (1997) 369–379. DOI: 10.1016/S0038-092X(97)00086-8

[14] R.B. Holdridge, D.C. Taff, Modular passive solar energy heating unit employing phase change heat storage material which is clearly transparent when in its high-stored-energy liquid state. U.S. Patent US4532917 A, 1985.

[15] L.A. Diaz, R. Viskanta, Experiments and analysis on the melting of a semitransparent material by radiation, Wärme- Und Stoffübertragung 20 (1986) 311–321.

[16] GLASSX, www.glassx.ch.

[17] H. Weinläder, A. Beck, J. Fricke, PCM-facade-panel for daylighting and room heating, Sol Energy 78 (2005) 177–186. DOI: 10.1016/j.solener.2004.04.013.

[18] F. Goia, M. Perino, V. Serra, Experimental analysis of the energy performance of a full-scale PCM glazing prototype, Sol Energy 100 (2014) 217–233. DOI: 10.1016/j.solener.2013.12.002.

[19] F. Goia, M. Perino, V. Serra, Improving thermal comfort conditions by means of PCM glazing systems, Energy Build 60 (2014) 442–452. DOI: 10.1016/j.enbuild.2013.01.029.

[20] F. Goia, M. Perino, M. Haase, A numerical model to evaluate the thermal behaviour of PCM glazing system configurations, Energy Build 54 (2012) 141–153. DOI: 10.1016/j.enbuild.2012.07.036

[21] F.C. Porisini, Salt hydrates used for latent heat storage: corrosion of metals and reliability of thermal performance. Sol Energy 41 (1988) 193–197. DOI: 10.1016/0038-092X(88)90136-3

[22] H. Manz, Sonnenstrahlungsbeladene Latentwärmespeicher in Gebäudefassaden, ETH - Swiss Federal Institute of Technology, 1996 *(in German)*.

[23] H. Weinläder, Optische Charakterisierung von Latentwärmespeichermaterialien zur Tageslichtnutzung. Universität Würzburg, 2003 *(in German)*.

[24] B.L. Gowreesunker, S.B. Stankovic, S.A. Tassou, P.A. Kyriacou, Experimental and numerical investigations of the optical and thermal aspects of a PCM-glazed unit, Energy Build 61 (2013) 239–249. DOI: 10.1016/j.enbuild.2013.02.032.

[25] ISO 9050:2003 – Glass in building – Determination of light transmittance, solar direct transmittance, total solar energy transmittance, ultraviolet transmittance and related glazing factors.

[26] A. Maccari, M. Montecchi, F. Treppo, M. Zinzi, CATRAM: An apparatus for the optical characterization of advanced transparent materials, Applied Optics 37 (1998) 5156–5161

[27] F. Goia, M. Perino, V. Serra, F. Zanghirella, Analisi sperimentale di un componente vetrato responsivo con materiali a cambiamento di fase, In: Atti del 65° Congresso Nazionale ATI, Domus de Maria (CA), 13-17 Settembre 2010. 1-8, ref. 09.275 *(in Italian)*.

TABLES

Table 1. *Optical characteristics of 4mm extra-clear glass pane used in the PCM glazing units*

Glass pane	δ_{PANE}	τ_e	ρ_e	α_e	τ_v	ρ_v	α_v
	mm	[-]	[-]	[-]	[-]	[-]	[-]
Extra-clear	4	0.91	0.08	0.01	0.92	0.08	0.00

Table 2. *Broad band light and solar properties of the samples for PCM in solid state recorded with commercial spectrophotometer (direct-to-hemisphere and direct-to-direct/specular mode)*

Glazed unit	δ_{PCM}	τ_e	$\tau_{e\rightarrow}$	ρ_e	$\rho_{e\rightarrow}$	α_e	τ_v	$\tau_{v\rightarrow}$	ρ_v	$\rho_{v\rightarrow}$	α_v
	[mm]	[-]	[-]	[-]	[-]	[-]	[-]	[-]	[-]	[-]	[-]
4 / 6 / 4	6	0.11	0.00	0.12	0.05	0.77	0.13	0.00	0.14	0.05	0.73
4 / 15 / 4	15	0.03	0.00	0.10	0.05	0.87	0.04	0.00	0.12	0.05	0.84
4 / 27 / 4	27	0.02	0.00	0.08	0.05	0.90	0.03	0.00	0.09	0.05	0.88

Table 3. *Integral (near) normal optical properties for different PCM layer thicknesses on the solar, visual and nir spectra, for the liquid and solid state*

State of aggregation	δ	τ_e	τ_v	τ_{nir}	ρ_e	ρ_v	ρ_{nir}	α_e	α_v	α_{nir}
[-]	[mm]	[-]	[-]	[-]	[-]	[-]	[-]	[-]	[-]	[-]
Liquid	15	0.75	0.85	0.62	0.09	0.09	0.08	0.17	0.06	0.32
Solid	6	0.46	0.54	0.36	0.28	0.34	0.21	0.27	0.12	0.45
	15	0.46	0.55	0.35	0.26	0.33	0.18	0.30	0.14	0.49
	27	0.37	0.46	0.25	0.25	0.30	0.18	0.35	0.19	0.56

Table 4. *Integral angular optical properties for PCM δ = 15mm (solid state) on the solar, visual and NIR spectra*

State of aggregation	δ	τ_e	τ_v	τ_{nir}	ρ_e	ρ_v	ρ_{nir}	α_e	α_v	α_{nir}
[-]	[deg]	[-]	[-]	[-]	[-]	[-]	[-]	[-]	[-]	[-]
Solid	0 (8)	0.46	0.55	0.35	0.26	0.33	0.18	0.30	0.14	0.49
	30	0.43	0.52	0.32	0.27	0.34	0.18	0.31	0.15	0.50
	45	0.41	0.50	0.30	0.27	0.34	0.19	0.32	0.16	0.51

Table 5. *Integral angular transmittance, for PCM δ = 6, 15 and 27 mm on the solar, visual and NIR spectra, for different beam angles, in both liquid and solid state*

	Solid state									*Liquid state*		
	6 mm			*15 mm*			*27 mm*			*15 mm*		
θ	τ_e	τ_l	τ_{nir}	τ_e	τ_l	τ_{nir}	τ_e	τ_l	τ_{nir}	τ_e	τ_l	τ_{nir}
[deg]	[-]	[-]	[-]	[-]	[-]	[-]	[-]	[-]	[-]	[-]	[-]	[-]
0 (8)	0,46	0,54	0,36	0,46	0,55	0,35	0,37	0,46	0,25	0,75	0,85	0,62
30	0,46	0,54	0,35	0,43	0,52	0,32	0,34	0,43	0,23	0,74	0,84	0,61
45	0,44	0,53	0,33	0,41	0,50	0,30	0,33	0,42	0,22	0,72	0,82	0,59

FIGURES' CAPTIONS

Figure 1. *Two of the PCM glazing samples, with PCM in solid state (left) and PCM in liquid state (right)*

Figure 2. *Optical bench apparatus in transmittance (top,) reflectance (mid) and absorptance (bottom) modes. Main parts: 1-light source; 2-integrating sphere (75 cm diameter); 3-optic fiber connected to the detection system; 4-sample port (transmittance port) with holder; 5-auxiliary port; 6-reflectance port with holder; 7-sample.*

Figure 3. *Spectral transmittance in the full range of value [τ: 0-1] (left) and a zoom in the range [τ: 0-0.2] (right) of the three DGUs with PCM recorded with a commercial spectrophotometer (PCM in solid state).*

Figure 4. *Spectral reflectance in the full range of value [τ: 0-1] (left) and a zoom in the range [τ: 0-0.2] (right) of the three DGUs with PCM recorded with a commercial spectrophotometer (PCM in solid state).*

Figure 5. *Spectral transmission coefficients of a 15mm PCM layer (DGU_PCM) in solid and liquid state (left), and spectral transmission coefficients of a 6mm, 15 mm and 27mm PCM layer (DGU_PCM) in solid state*

Figure 6. *Spectral reflection coefficients of a 15mm PCM layer (DGU_PCM) in solid and liquid state (left), and spectral reflection coefficients of a 6mm, 15 mm and 27mm PCM layer (DGU_PCM) in solid state*

Figure 7. *Spectral absorption coefficients of a 15mm PCM layer (DGU_PCM) in solid and liquid state (left), and spectral absorption coefficients of a 6mm, 15 mm and 27mm PCM layer (DGU_PCM) in solid state*

Figure 8. *Spectral transmission coefficients of a 15mm PCM layer (DGU_PCM) in liquid state (left) and solid state (right), for different incident beam angles (0 deg, 30 deg, 45 deg).*

Figure 9. *Spectral transmission coefficients of a 6 mm PCM layer (DGU_PCM) in solid state (left) and of a 27 mm PCM layer (DGU_PCM) in solid state state (right), for different incident beam angles (0 deg, 30 deg, 45 deg).*

Figure 10. *Spectral absorption coefficients of a 15 mm PCM layer (DGU_PCM) in solid state (for different incident beam angles (0 deg, 30 deg, 45 deg).*

mage

Figure 2
Click here to download high resolution image

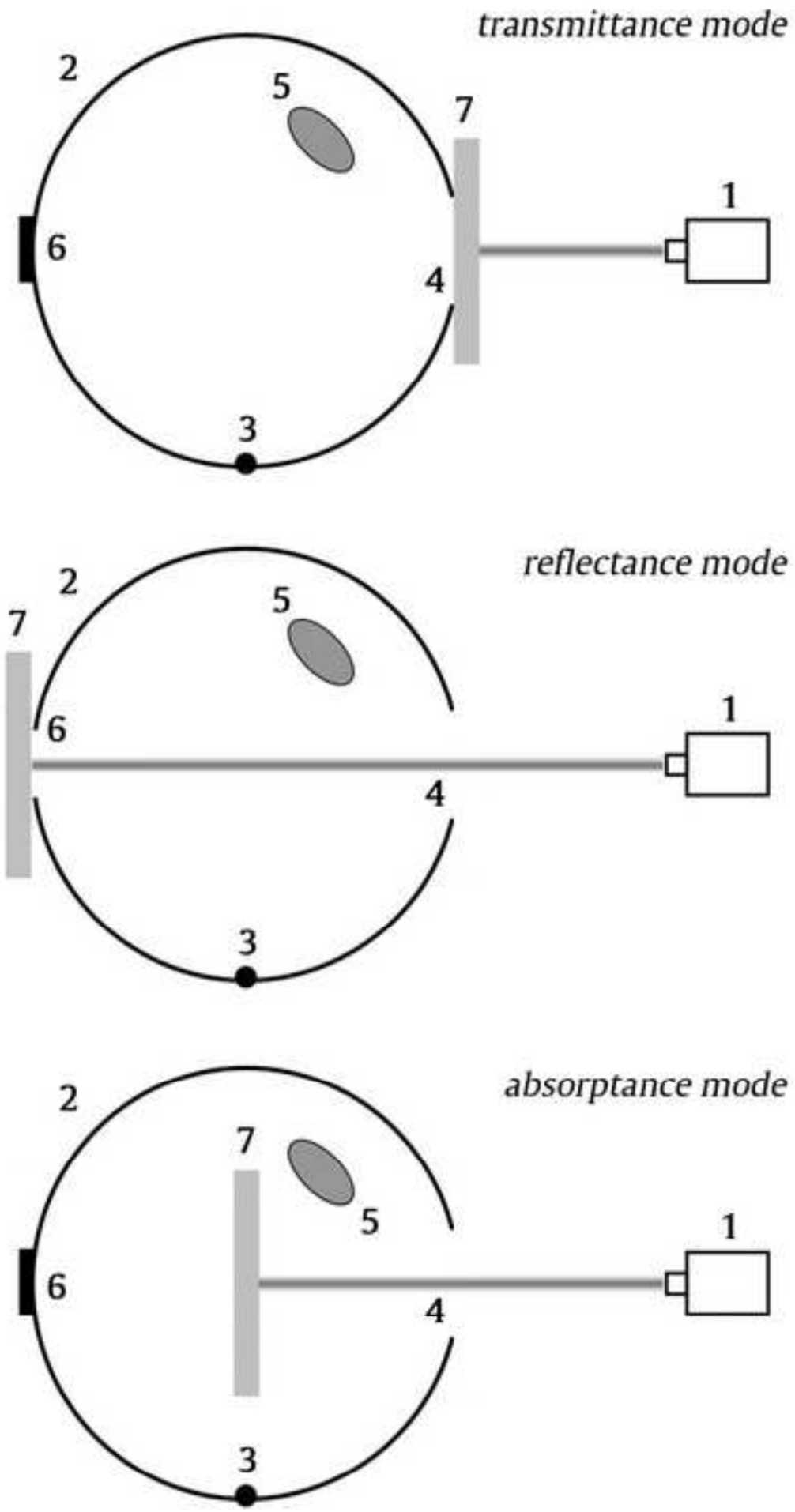

mage

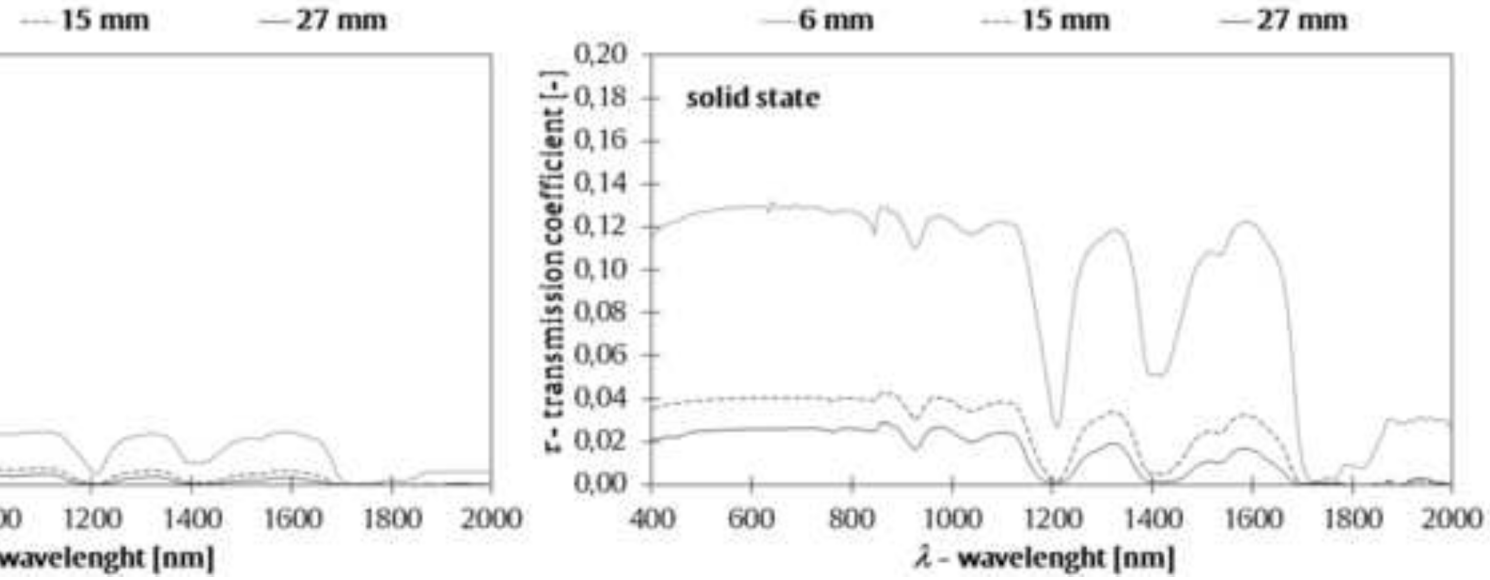
15 mm
27 mm
1200
1400
1600
1800
2000
wavelenght [nm]
6 mm
15 mm
27 mm
solid state
τ - transmission coefficient [-]
0,20
0,18
0,16
0,14
0,12
0,10
0,08
0,06
0,04
0,02
0,00
400
600
800
1000
1200
1400
1600
1800
2000
λ - wavelenght [nm]

mage

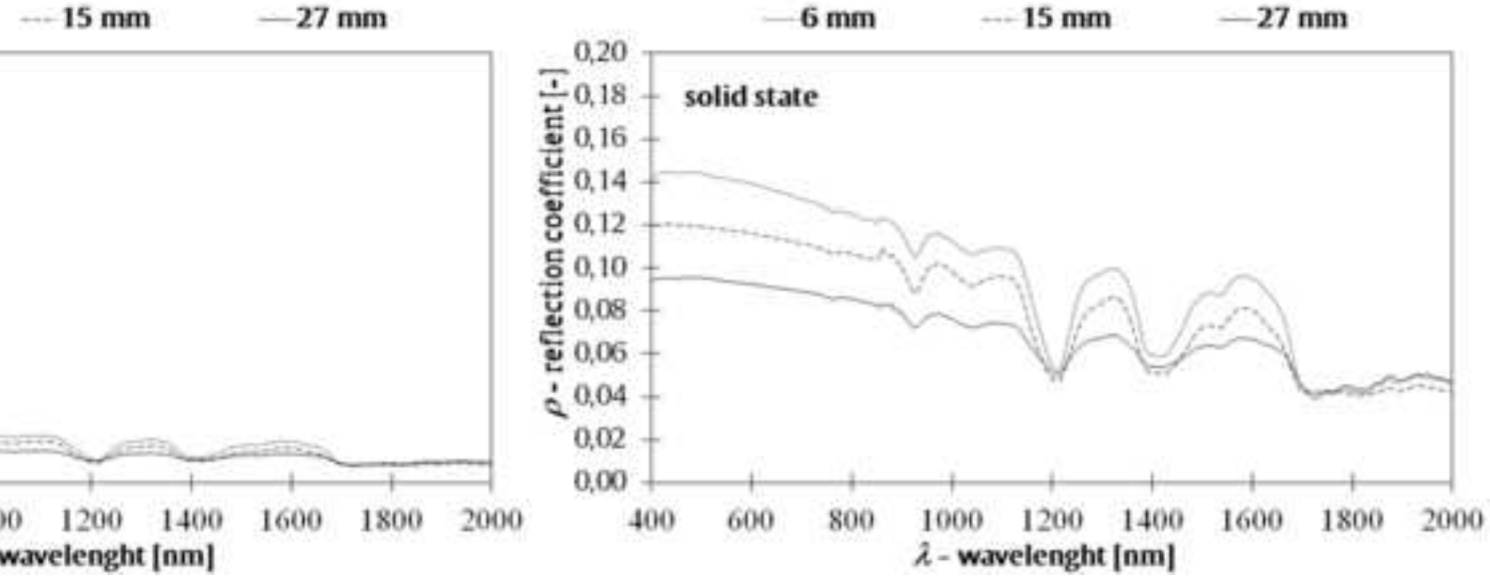
15 mm
27 mm
wavelenght [nm]
6 mm
15 mm
27 mm
solid state
ρ - reflection coefficient [-]
0,20
0,18
0,16
0,14
0,12
0,10
0,08
0,06
0,04
0,02
0,00
400
600
800
1000
1200
1400
1600
1800
2000
λ - wavelenght [nm]

mage

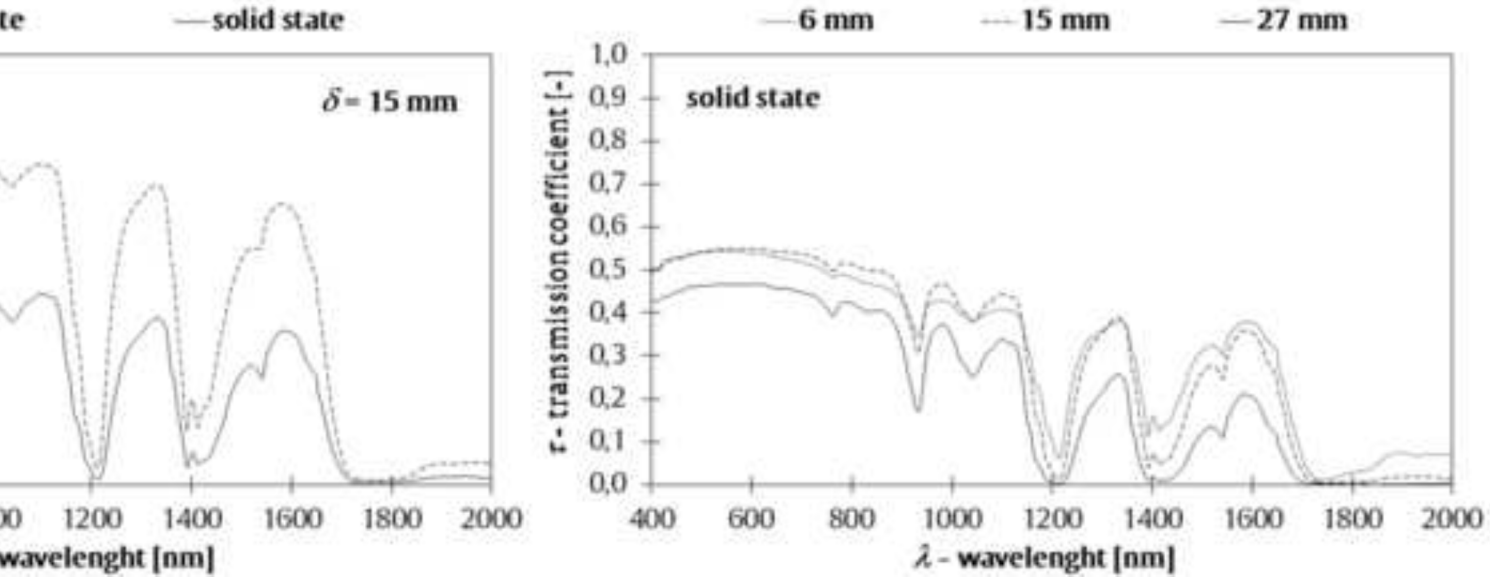
te
solid state
δ = 15 mm
00 1200 1400 1600 1800 2000
wavelenght [nm]
6 mm
15 mm
27 mm
solid state
τ - transmission coefficient [-]
1,0
0,9
0,8
0,7
0,6
0,5
0,4
0,3
0,2
0,1
0,0
400 600 800 1000 1200 1400 1600 1800 2000
λ - wavelenght [nm]

mage

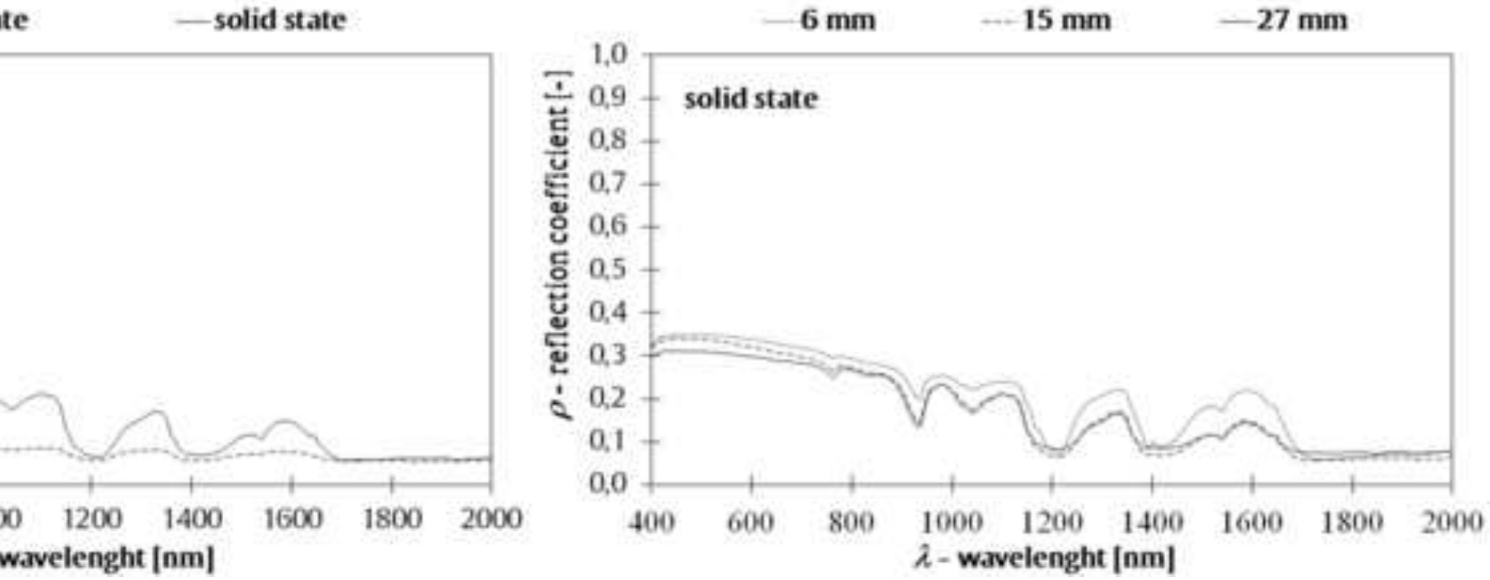
te
solid state
00 1200 1400 1600 1800 2000
wavelenght [nm]
6 mm
15 mm
27 mm
solid state
ρ - reflection coefficient [-]
1,0
0,9
0,8
0,7
0,6
0,5
0,4
0,3
0,2
0,1
0,0
400 600 800 1000 1200 1400 1600 1800 2000
λ - wavelenght [nm]

mage

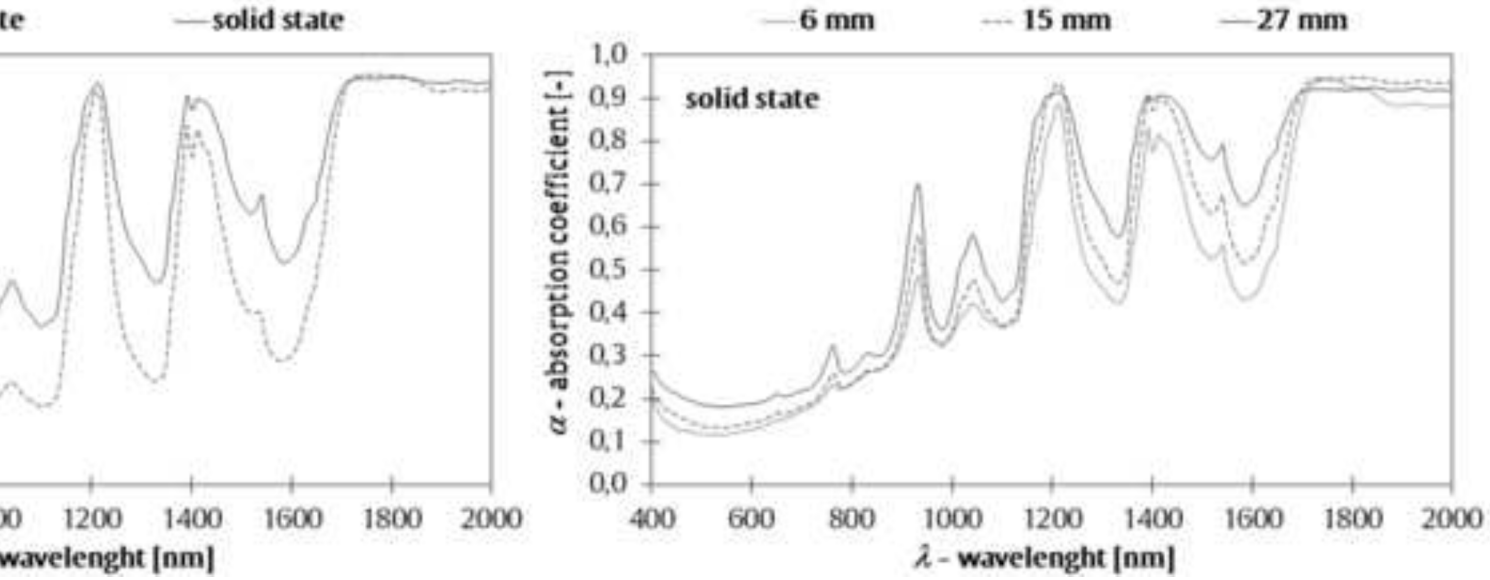
te
solid state
00 1200 1400 1600 1800 2000
wavelenght [nm]
6 mm
15 mm
27 mm
solid state
α - absorption coefficient [-]
1,0
0,9
0,8
0,7
0,6
0,5
0,4
0,3
0,2
0,1
0,0
400 600 800 1000 1200 1400 1600 1800 2000
λ - wavelenght [nm]

mage

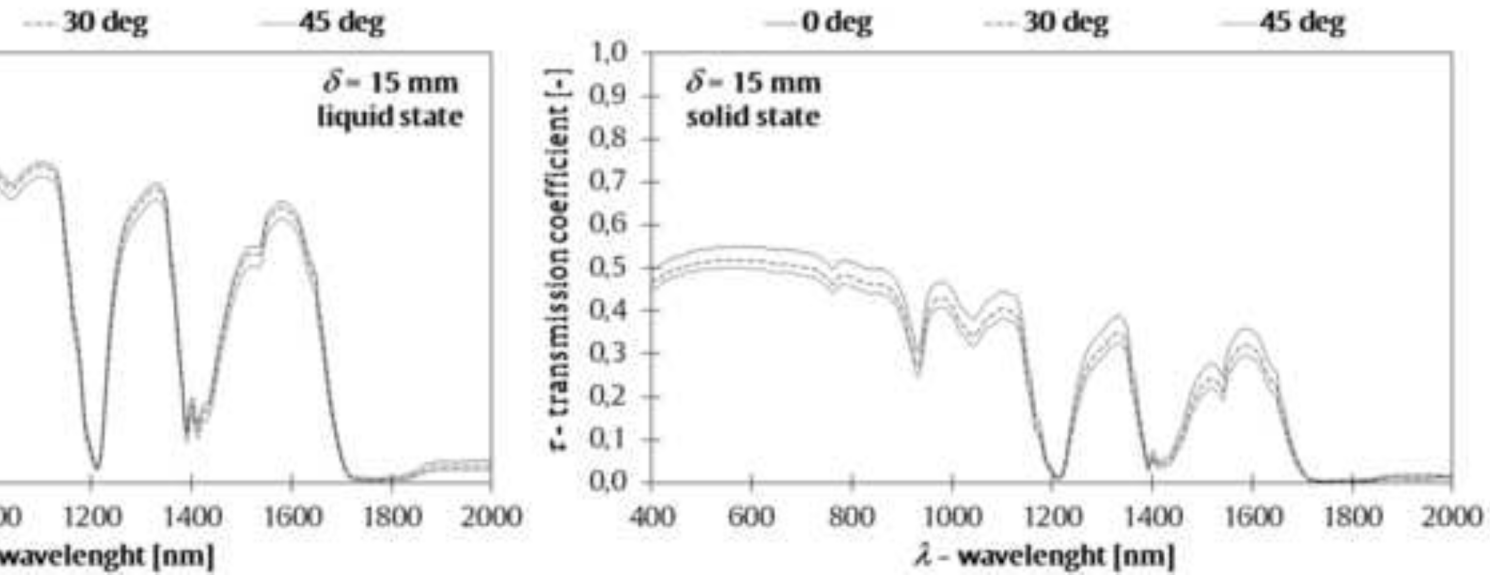
30 deg
45 deg
δ = 15 mm
liquid state
1200
1400
1600
1800
2000
wavelenght [nm]
0 deg
30 deg
45 deg
δ = 15 mm
solid state
τ - transmission coefficient [-]
1,0
0,9
0,8
0,7
0,6
0,5
0,4
0,3
0,2
0,1
0,0
400
600
800
1000
1200
1400
1600
1800
2000
λ - wavelenght [nm]

mage

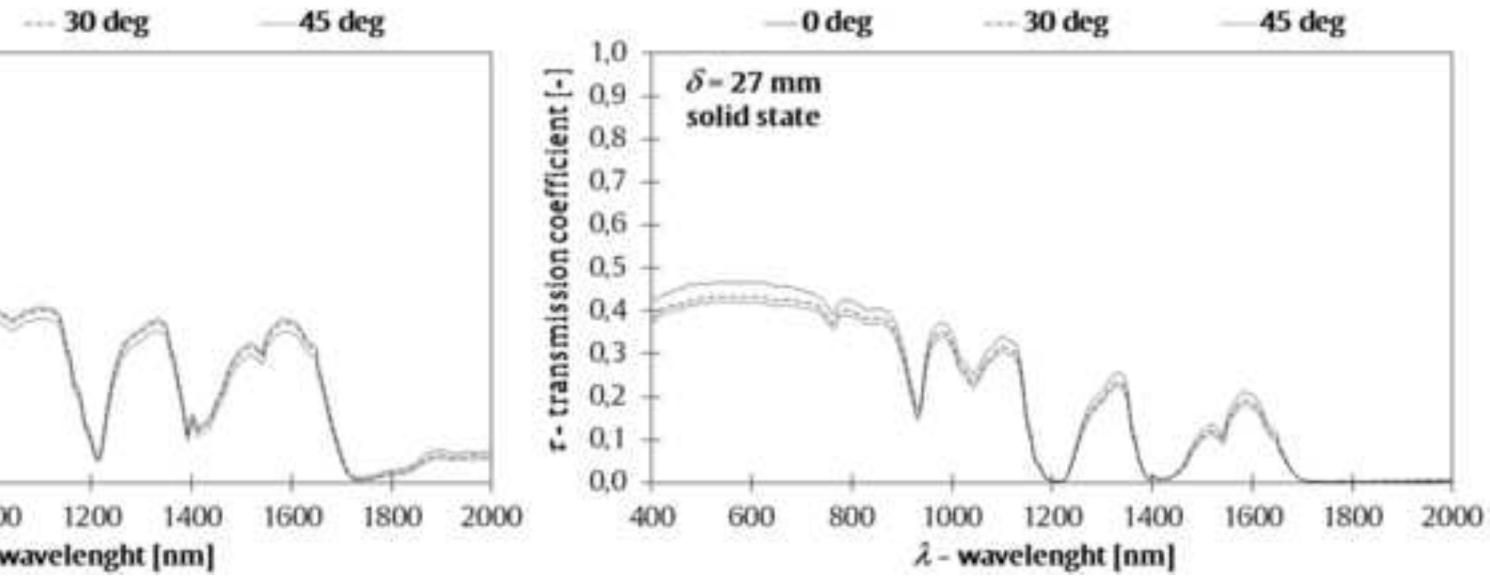
30 deg
45 deg
1200
1400
1600
1800
2000
wavelenght [nm]
0 deg
30 deg
45 deg
τ - transmission coefficient [-]
1,0
0,9
0,8
0,7
0,6
0,5
0,4
0,3
0,2
0,1
0,0
δ = 27 mm
solid state
400
600
800
1000
1200
1400
1600
1800
2000
λ - wavelenght [nm]

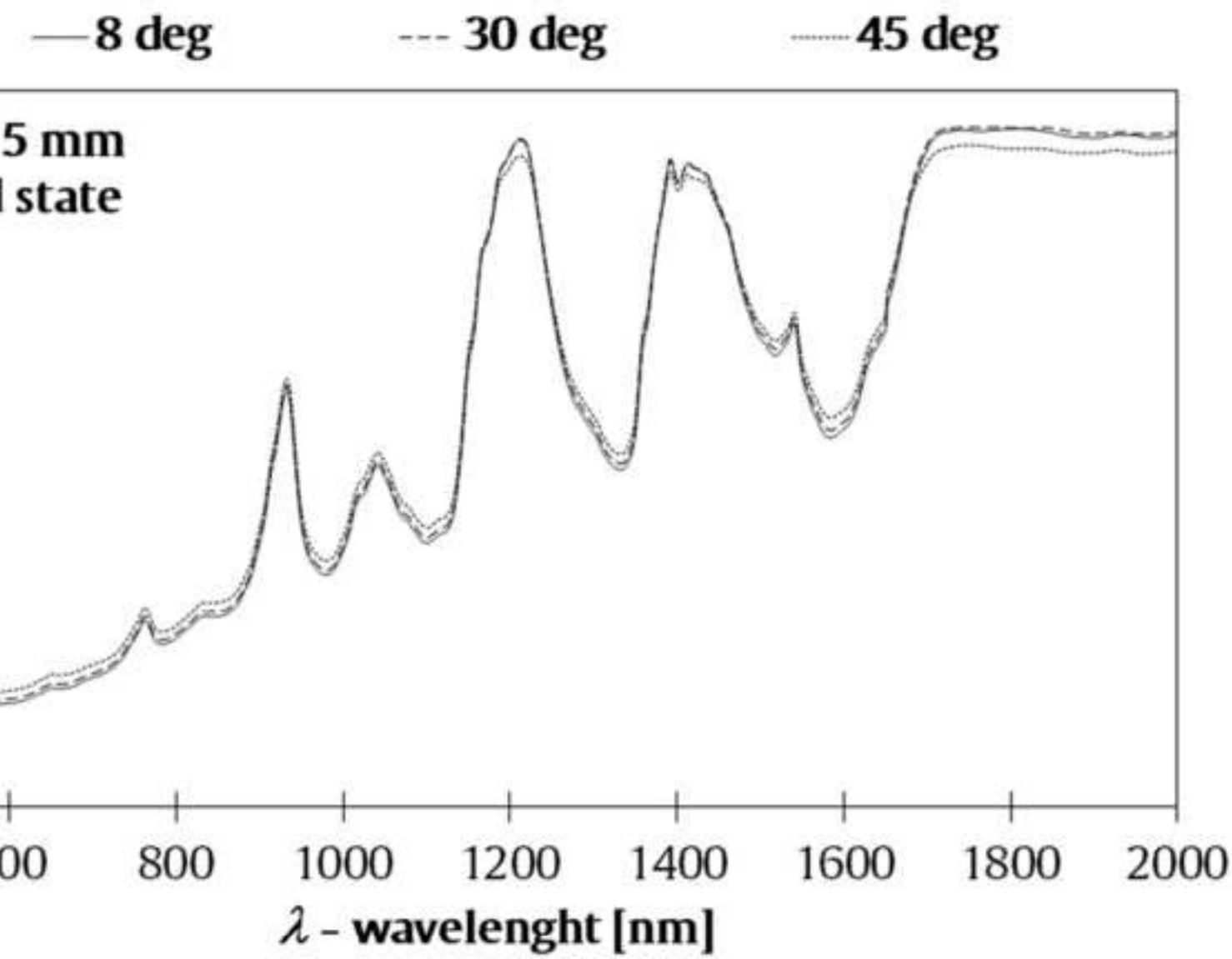
8 deg
30 deg
45 deg
5 mm
state
00
800
1000
1200
1400
1600
1800
2000
λ - wavelenght [nm]